Manipulation of tripartite frequency correlation under extended phase matchings

Qun-Yong Zhang,[1,2] Guang-Tai Xue,[1] Ping Xu,[1,3,*] Yan-Xiao Gong,[1] Zhenda Xie,[4] and Shining Zhu[1]

[1]*National Laboratory of Solid State Microstructures and School of Physics, Nanjing University, Nanjing 210093, People's Republic of China*

[2]*Faculty of Mathematics and Physics, Huaiyin Institute of Technology, Huaian 223003, People's Republic of China*

[3]*Institute for Quantum Information and State Key Laboratory of High Performance Computing, College of Computing, National University of Defense Technology, Changsha 410073, People's Republic of China*

[4]*National Laboratory of Solid State Microstructures and School of Electronic Science and Engineering, Nanjing University, Nanjing 210093, People's Republic of China*

(Received 23 November 2017; published 20 February 2018)

We investigate how to manipulate the tripartite frequency correlation of triplets which are generated from cascaded spontaneous parametric down-conversions. A monolithic quadratic nonlinear crystal is designed to contain two segments of periodically poled lithium niobate waveguide as nonlinear mediums to produce cascaded photon pairs both under phase-matching and group-velocity-matching conditions. By choosing proper pump bandwidth and crystal length, the tripartite frequency will show a full correlation, partial correlation, or no correlation, corresponding an inseparable triplet, separable one photon and biphoton, or three separable photons, respectively. This opens up a way to manipulate the tripartite correlation, which is important for understanding quantum fundamentals and also can supply key elements for developing new quantum technologies.

DOI: 10.1103/PhysRevA.97.022327

I. INTRODUCTION

Quantum correlations between individual particles lie at the heart of quantum mechanics and supply the basis to build various quantum technologies [1]. To construct quantum correlation between two particles, one of the most common methods is to adopt the spontaneous parametric down-conversion (SPDC) process during which a photon from a pump laser beam can spontaneously be converted into a pair of signal-idler photons when the pump photon is incident into a nonlinear optical medium. The conservation of the total energy and momentum, known as phase matching, leads to strong correlations between the generated photon pair which can be used to produce quantum entanglement over a variety of degrees of freedom and find applications for different quantum technologies. Taking the two-photon energy-time correlation as the example, two photons will show anticorrelation, positive correlation, or no correlation when the SPDC is properly designed. Energy anticorrelated photons can be used to alleviate the deleterious effects of dispersion in quantum cryptography [2] and the potential damage to sensitive biological samples [3]. Frequency-uncorrelated photons are desired because they provide a heralded source of pure-state photons [4–6], which is an important tool in quantum information processing. Quantum enhanced position and clock synchronization techniques require frequency-correlated photon pairs [7–9] which can be generated from pulsed pump laser under extended phase-matching (EPM) conditions.

Quantum correlation between three or more particles will show complex yet interesting characteristics. Many efforts have been concentrated on generating multipartite entanglement for its wide variety of applications in quantum computation [10,11] and communication networks [12,13]. A popular and rapidly developing method to prepare multiphoton entanglement is based on the indistinguishable yet independent photon pairs generated from SPDC when pumped by a femtosecond laser, but in a postselected way [14,15]. This method has been experimentally approved as an reliable and valuable source for prompting the practical use of quantum computing [16,17] or demonstration of quantum supremacy by boson sampling [18–21]. A different strategy for preparing multiphoton entanglement without postselection is based on the cascaded SPDCs. One of the photons from the first SPDC acts as the pump photon and is converted into a pair of photon in a cascaded way. The remaining photon from the first SPDC and the cascaded photon pair from the second SPDC constitute a triplet. The photon triplet originates from a single-pump photon, so the energy and momentum obey strong correlations, unlike the aforementioned independent pairs. Until 2010, the first triplet was experimental observed by Hübel *et al.* [22], although it was proposed in 1990 [23]. The same group also verified the tripartite photons share strong spectral correlation and exhibit genuine entanglement in the frequency-time regime [24,25] as well as in the polarization degree of freedom [26]. Their experimental results have proven the feasibility of generating heralded Bell states with high visibility and fidelity, but without the need for postselection. Based on the idea of cascaded SPDC, Krapick *et al.* designed and fabricated a monolithic photon-triplet source in a second-order nonlinear waveguide chip [27], and their results make crucial progress toward a robust, scalable, and miniaturized quantum technology. Unlike the cascaded second-order nonlinear processes, photon triplets generated by third-order nonlinearity [28,29] are derived from a single event in which one pump photon is annihilated to generate three signal photons.

*pingxu520@nju.edu.cn

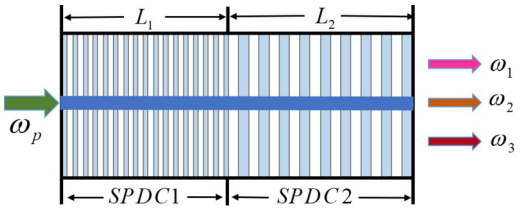

FIG. 1. Schematic of the cascaded periodically poled crystal. Triplets at frequencies ω_1, ω_2, and ω_3 are generated by cascaded SPDC processes driven by a pump at frequency ω_p. Λ_1 and Λ_2 are the poled periods of the corresponding two segments with lengths L_1 and L_2, respectively.

Although the triplet generated by cascaded SPDC has been observed and the genuine energy-time entanglement over three photons has been verified, the engineering of tripartite frequency correlation of the triplet is left undisclosed and different types of tripartite correlations deserve to be characterized. In this paper, we design the cascaded SPDC under EPM conditions to tailor the triplet spectrum, resulting in a mutable tripartite correlation. Transitions among a full tripartite correlation, partial correlation, or no correlation are achieved, corresponding an inseparable triplet, separable one photon, and biphoton or three separable photons, respectively. This opens up a way to manipulate the tripartite correlation, which is important for understanding quantum fundamentals and stimulating the development of new quantum technologies.

II. TRIPARTITE STATE AND JOINT SPECTRUM

A. Description of nonlinear medium for cascaded SPDC in our scheme

In our scheme, the generation of three photons is the same as in Ref. [22], but we suggest integrating the cascaded SPDC processes on a monolithic periodically poled crystal waveguide just like in Ref. [27] to increase the efficiency of triplet by avoiding the interface loss between two SPDCs. In periodically poled crystal, quasi-phase-matching (QPM) ensures the momentum conservation among the pump, signal, and idler in a flexible way, which has been extensively studied in quantum optics field to build efficient sources for producing entanglement because its unique advantages [30–33], such as higher efficiency over birefringence phase matching (BPM), enables flexible frequency-tunable and collinear nonlinear processes. Here in this work, the single quadratic nonlinear crystal waveguide contains two poling segments, as Fig. 1 shows. The lengths (periods) of two segments are L_1 and L_2 (Λ_1 and Λ_2), respectively. The modulated nonlinearity susceptibilities with positive χ and negative $-\chi$ are interchanged from one to another.

A pump photon with central frequency ω_p will occasionally split into a pair of signal-idler photons with frequencies ω_1 and ω_0 in the first nondegenerate SPDC process. Then this process is repeated with photon ω_0, now serving as the pump in the second SPDC area, creating simultaneously a pair of new photons with frequencies ω_2 and ω_3. The energy conservation condition must be fulfilled in the two processes, i.e., $\omega_p = \omega_1 + \omega_0$, $\omega_0 = \omega_2 + \omega_3$, and then we have $\omega_p = \omega_1 + \omega_2 + \omega_3$, which indicate that the total energies of triplet equal to that of original pump laser. Likewise, the conservation of momentum which is usually referred to as phase-matching condition also needs to be satisfied. By periodically inverting the nonlinear susceptibility in the two different segments, we create rectangular quadratic gratings with the corresponding reciprocal vectors $g_1 = 2\pi/\Lambda_1$, $g_2 = 2\pi/\Lambda_2$. We include this in the momentum conservation condition, which can be expressed as $k_p = k_1 + k_0 + g_1, k_0 = k_2 + k_3 + g_2$. Then we have that $k_p = k_1 + k_2 + k_3 + g_1 + g_2$. This indicates that the total momenta of the triplets are conserved. We restrict our analysis here only collinear, one-dimensional propagation configurations in the periodically poled crystal waveguide. A simple method to spatially separate the collinear photon triplets at the output is by using dichroic mirrors, because the triplets are generated by nondegenerate SPDC processes at substantially different frequencies.

B. Derivation of tripartite state

In this subsection, we will formulate the photon triplet generated by cascaded SPDC. In the interaction picture, the effective Hamiltonian for one SPDC process in a nonlinear crystal may be written as

$$H_I = \varepsilon_0 \int dV \chi^{(2)} E_p^{(+)} E_s^{(-)} E_i^{(-)} + \text{H.c.}, \tag{1}$$

where ε_0 is the vacuum permittivity, $\chi^{(2)}$ is the second-order susceptibility of the medium, the integral is taken over the interaction volume V, and H.c. stands for Hermitian conjugate. $E_j^{(+)}$ and $E_j^{(-)}$ are positive- and negative-frequency components of the field operators of the signal and idler, respectively, expressed as

$$E_j^{(-)} = \int d\omega_j E^*(\omega_j) e^{-i(k_j \cdot r - \omega_j t)} \hat{a}^\dagger_{(\omega_j)}, \tag{2}$$

where $E_{(\omega_j)} = i\sqrt{\hbar\omega_j/4\pi\varepsilon_0 c n^2_{(\omega_j)} S}$, $(j = s,i)$, $E^{(+)} = (E^{(-)})^\dagger$, and $a^\dagger(\omega_j)$ is the photon creation operator of frequency ω at the jth detector and obeys commutation relation $[a_j(\omega), a_k^\dagger(\omega')] = \delta(\omega - \omega')\delta_{j,k}$. The first SPDC stage is pumped with a classical field $E_p^{(+)}$ which has the form

$$E_p^{(+)} = \int d\omega_p \tilde{E}(w_p) e^{i(k_p \cdot r - \omega_p t)}. \tag{3}$$

Consider that the pump, centered at Ω_p, with pulse bandwidth σ, has a Gaussian spectral envelope $\tilde{E}(\omega_p) = E_0 \exp[-(\omega_p - \Omega_p)^2/\sigma^2]$. The total Hamiltonian of the cascaded SPDC processes in a monolithic crystal can be written as

$$H = H_I^{(1)} + H_I^{(2)} = \varepsilon_0 \int \chi_1^{(2)} dV_1 E_p^{(+)} E_0^{(-)} E_1^{(-)} + \varepsilon_0 \int \chi_2^{(2)} dV_2 E_0^{(+)} E_2^{(-)} E_3^{(-)} + \text{H.c.}, \tag{4}$$

$H_I^{(1)}$, $H_I^{(2)}$ are the Hamiltonian for the first and second SPDC process, respectively. The unitary evolution of a state vector from time t' to t'' in the absence of propagation loss can be

expressed as

$$|\Psi\rangle = \exp\left[\frac{1}{i\hbar}\int_{t'}^{t''} dt\, H_I(t)\right]|0\rangle = |0\rangle + \frac{1}{i\hbar}\int_{t'}^{t''} dt\, H_I(t)|0\rangle + \frac{1}{2!}\left(\frac{1}{i\hbar}\right)^2 \int dt_1 dt_2 H(t_1)H(t_2)|0\rangle + \cdots, \quad (5)$$

where $|0\rangle$ is the vacuum, the tripartite state arising from the third term of the Taylor series expansions, which can be written as

$$|\Phi\rangle = C_0 \int dt_1 dt_2 dz_1 dz_2 E_0^{(+)} E_2^{(-)} E_3^{(-)} E_p^{(+)} E_1^{(-)} E_0^{(-)}|0\rangle. \quad (6)$$

Then, by substituting Eqs. (2) and (3) into Eq. (6), we obtain

$$|\Phi\rangle = C_0 \int d\omega_p d\omega_0 d\omega_1 d\omega_2 d\omega_3 \exp\left[-\frac{(\omega_p-\Omega_p)^2}{\sigma^2}\right] \times \int_0^{L_2} dz_2 e^{i(k_0-k_2-k_3-g_2)z_2} \int_{-L_1}^{0} dz_1 e^{i(k_p-k_0-k_1-g_1)z_1} \times \int dt_2 e^{-i(\omega_0-\omega_2-\omega_3)t_2} \int dt_1 e^{-i(\omega_p-\omega_1-\omega_0)t_1} a_1^\dagger a_2^\dagger a_3^\dagger |0\rangle. \quad (7)$$

All constant factors have been lumped into C_0 in the above equations. Considering steady-state output, we may set $t' = -\infty$ and $t'' = \infty$, and then we have

$$\int_{-\infty}^{\infty} dt_1 e^{-i(\omega_0-\omega_2-\omega_3)t_1} = 2\pi\delta(\omega_0-\omega_2-\omega_3),$$
$$\int_{-\infty}^{\infty} dt_2 e^{-i(\omega_p-\omega_1-\omega_0)t_2} = 2\pi\delta(\omega_p-\omega_1-\omega_0), \quad (8)$$

which give the energy conservation condition $\omega_p - \omega_1 - \omega_2 - \omega_3 = 0$. Integrating over the finite length of the crystal L_1 and L_2 give the longitudinal detuning function, which determines the natural spectral width of the photon triplets

$$\int_{-L_1}^{0} dz_1 e^{-i\Delta k_1 z_1} = L_1 e^{-i\frac{\Delta k_1 L_1}{2}} \operatorname{sinc}\frac{\Delta k_1 L_1}{2},$$
$$\int_{0}^{L_2} dz_2 e^{-i\Delta k_2 z_2} = L_2 e^{-i\frac{\Delta k_2 L_2}{2}} \operatorname{sinc}\frac{\Delta k_2 L_2}{2}, \quad (9)$$

where $\Delta k_1 = k_p - k_0 - k_1 - g_1$ and $\Delta k_2 = k_0 - k_2 - k_3 - g_2$. As a result, the final expression for the state vector is

$$|\Phi\rangle = C_1 \int d\omega_1 d\omega_2 d\omega_3 e^{-i\frac{(\Delta k_1 L_1 + \Delta k_2 L_2)}{2}} e^{-\frac{(\omega_p-\Omega_p)^2}{\sigma^2}} \times \operatorname{sinc}\left(\frac{\Delta k_1 L_1}{2}\right)\operatorname{sinc}\left(\frac{\Delta k_2 L_2}{2}\right) a_{\omega_1}^\dagger a_{\omega_2}^\dagger a_{\omega_3}^\dagger |0\rangle. \quad (10)$$

In the case of nondegenerate type-I processes, because of the existence of the bandwidth, we can define $\omega_j = \Omega_j + \nu_j$, where ν_j $(j = p,1,2,3)$ is the detuning from the central frequency Ω_j. Note that $\Omega_p = \Omega_1 + \Omega_2 + \Omega_3$, $\nu_p = \nu_1 + \nu_2 + \nu_3$, the wave numbers $k_j = n_{(\omega_j)}\omega_{(j)}/c$, where $n_{(\omega_j)}$ is the effective index of refraction of the crystal waveguide at frequency $\omega_{(j)}$, and c is the speed of light. Now we can expand the wave vectors around the central frequencies up to first order in detuning ν_j. Then δ_k can be written as

$$\delta_k = k_p - k_s - k_i - g = (k_{\Omega_p} - k_{\Omega_s} - k_{\Omega_i} - g) + \left(\frac{\nu_p}{\mu_p} - \frac{\nu_s}{\mu_s} - \frac{\nu_i}{\mu_i}\right), \quad (11)$$

where $\mu_j = d\omega_j/dk_j$ are the group velocities of the photons at central frequencies Ω_j. Suppose the perfect phase-matching conditions can be satisfied at the central frequency; therefore, according to the following QPM conditions for the two collinear SPDC processes:

$$k_{\Omega_p} - k_{\Omega_0} - k_{\Omega_1} - g_1 = 0,$$
$$k_{\Omega_0} - k_{\Omega_2} - k_{\Omega_3} - g_2 = 0. \quad (12)$$

Then the zeroth-order terms in the expansion vanish, giving

$$\Delta k_1 = \left(\frac{1}{\mu_p} - \frac{1}{\mu_1}\right)\nu_1 + \left(\frac{1}{\mu_p} - \frac{1}{\mu_0}\right)\nu_2 + \left(\frac{1}{\mu_p} - \frac{1}{\mu_0}\right)\nu_3,$$
$$\Delta k_2 = \left(\frac{1}{\mu_0} - \frac{1}{\mu_2}\right)\nu_2 + \left(\frac{1}{\mu_0} - \frac{1}{\mu_3}\right)\nu_3. \quad (13)$$

For simplicity, we define the coefficients of ν_1,ν_2,ν_3 in Eq. (13) as $a_1 = 1/\mu_p - 1/\mu_1, a_2 = 1/\mu_p - 1/\mu_0, b_1 = 1/\mu_0 - 1/\mu_2, b_2 = 1/\mu_0 - 1/\mu_3$. Since it is difficult to integrate the products of Gaussians and sinc functions in Eq. (10), we have made use of the approximation in our calculation to express the sinc function as Gaussians through the approximation $\operatorname{sinc}(x) \approx \exp(-\gamma x^2)$, where the parameter $\gamma = 0.193$ is derived from equating the full-width half maximum of the two functions. In this way, we will obtain the triplet in an integral format of detuning variables:

$$|\Phi\rangle = C_1 \int d\nu_1 d\nu_2 d\nu_3 F(\nu_1,\nu_2,\nu_3) a_{\nu_1}^\dagger a_{\nu_2}^\dagger a_{\nu_3}^\dagger |0\rangle. \quad (14)$$

The spectral properties are fully determined by $F(\nu_1,\nu_2,\nu_3)$, which we refer to as the joint spectral amplitude (JSA) of the triplet wave function described as

$$F(\nu_1,\nu_2,\nu_3) = e^{-i(\Delta k_1 L_1 + \Delta k_2 L_2)/2} e^{-(\nu_1+\nu_2+\nu_3)^2/\sigma^2} \times e^{-\frac{\gamma L_1^2 a_1^2}{4}\left[\nu_1 + \frac{a_2}{a_1}(\nu_2+\nu_3)\right]^2} e^{-\frac{\gamma L_2^2 b_1^2}{4}\left(\nu_2 + \frac{b_2}{b_1}\nu_3\right)^2}. \quad (15)$$

III. FREQUENCY CORRELATION OF TRIPLETS UNDER EXTENDED PHASE MATCHING

In this section, we mainly discuss frequency correlation of triplets under EPM conditions. EPM requires that, besides the conversional phase-matching condition, group velocity matching (GVM) is also satisfied, as described in Refs. [8,9]. In order to manipulate the spectral properties of triplets, both the group velocity and the phase velocity are required to be matched simultaneously. It may be difficult for conventional BPM crystals, but it is competent for QPM in periodically poled materials since the reciprocal vector can be designed after the GVM condition is satisfied. However, this will constrain the EPM happening at a certain wavelength of a certain polarization configuration inside a certain QPM crystal. The contour of the joint spectral intensity (JSI) is

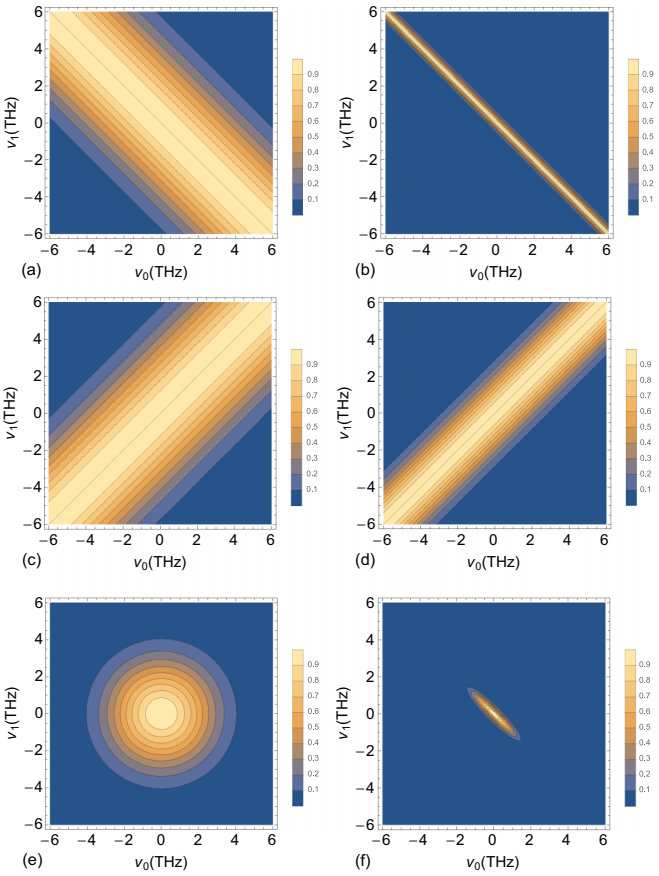

FIG. 2. [(a), (b)] The pump envelope intensity with the bandwidth $\sigma_a = 5.33$ THz, $\sigma_b = 0.533$ THz, respectively. [(c), (d)] The phase-matching intensity with the crystal length $L_c = 1$ cm, $L_d = 2$ cm; the subscripts denote the corresponding subfigure. Panels (e) and (f) correspond to the joint spectral intensity determined by panels (a) and (c) and panels (b) and (d), respectively.

determined by $|F(\nu_1,\nu_2,\nu_3)|^2$, which consists of the pump envelope intensity and phase matching intensity. Unlike the analysis in Refs. [34,35], the JSI of triplets consisted of two phase-matching functions and a pump envelope function.

We start our analysis by giving a description of frequency correlation between ν_0 and ν_1 generated in the first SPDC process. Depending on the relative widths of the pump function and phase-matching function, the JSI can be either anticorrelated, uncorrelated, or positively correlated. The width of the pump envelope intensity contour is proportional to the pump bandwidth, while the angle is fixed at 45 deg with the minus direction of the horizontal coordinate due to the energy conservation law. In other words, the pump envelope function itself tends to yield anticorrelation. Figures 2(a) and 2(b) show plots of pump envelope intensity. Gaussian shape has been assumed for the pump, and the values of bandwidth in Figs. 2(a) and 2(b) are $\sigma_a = 5.33$ THz and $\sigma_b = 0.533$ THz, respectively. The details of the other parameters we selected are described in Subsec. B. Figures 2(c) and 2(d) show plots of phase-matching intensity, where the width of the phase-matching intensity is related to the inverse of the crystal length. The angle between the phase-matching intensity contour and the horizontal coordinate is not fixed; it is decided by the group velocities of the pump, signal, and idler photons, i.e., the specific values of a_2/a_1 in Eq. (15). The crystal length L_d we choose in Fig. 2(d) is twice of the length L_c in Fig. 2(c), yet the width of the contour is just half. When the widths of the pump function and phase-matching function are similar and the angle of the phase matching intensity is at 45 deg [see Figs. 2(a) and 2(c)], the JSI can achieve a circular shape and the corresponding state has a low degree of entanglement as shown in Fig. 2(e). It shows anticorrelation between ν_0 and ν_1 in Fig. 2(f) when the width of the pump envelope intensity in Fig. 2(b) is more narrow than the width of the phase-matching intensity in Fig. 2(d), and positive correlation when the contour of phase matching intensity is more narrow.

A. Inseparable tripartite frequency correlation

Now we take the second SPDC process into consideration; ω_0 serves as the pump in the second segment, creating a pair of new photons with frequencies ω_2 and ω_3. Three photons with detuning frequencies ν_1, ν_2, and ν_3 share different frequency correlations under different conditions. If the crystal is pumped with a monochromatic continuous wavelength (cw) laser, i.e., $\sigma \to 0$, the sum of the frequencies of the down-converted photons is fixed, thus the frequencies of photons ω_0 and ω_1 are anticorrelated in the first SPDC stage. In this situation, a frequency measurement on one photon exactly determines the outcome of a frequency measurement on the other photon. Once the frequency ω_1 is fixed, the down-converted photons ω_2 and ω_3 in the second SPDC process are anticorrelated, although none of them are determined for their sum of frequencies is fixed at ω_0. To some extent, the inseparable triplet, generated via the cascaded parametric processes, pumped by a monochromatic cw laser or by a narrow-band laser, is naturally endowed with a specific form of strong frequency anticorrelation induced by the energy conservation law. The JSA of the nonseparable triplet can be written as

$$F(\nu_1,\nu_2,\nu_3) = e^{-\alpha\nu_1^2}e^{-\beta\nu_2^2}e^{-\eta\nu_3^2}e^{-\iota\nu_1(\nu_2+\nu_3)}e^{-\kappa\nu_2\nu_3}, \quad (16)$$

where $\alpha = 1/\sigma^2 + \gamma L_1{}^2 a_1{}^2/4$, $\beta = 1/\sigma^2 + \gamma L_1{}^2 a_2{}^2/4 + \gamma L_2{}^2 b_1{}^2/4$, $\eta = 1/\sigma^2 + \gamma L_1{}^2 a_2{}^2/4 + \gamma L_2{}^2 b_2{}^2/4$, $\iota = 2/\sigma^2 + \gamma L_1{}^2 a_1 a_2/2$, and $\kappa = 2/\sigma^2 + \gamma L_1{}^2 a_2{}^2/2 + \gamma L_2{}^2 b_1 b_2/2$. Figure 3 shows a plot of JSI of the triplet calculated by the formula $|F(\nu_1,\nu_2,\nu_3)|^2$ pumped by a narrow-band laser with a bandwidth of 5 MHz. Correlation between two subsystems ν_2 and ν_3 can be obtained by tracing out ν_1 in the tripartite state described as

$$I_{(\nu_2,\nu_3)} = \int d\nu_1 |F(\nu_1,\nu_2,\nu_3)|^2. \quad (17)$$

Following the same method, it is easy to plot frequency correlation contours between any two photons in the tripartite state. ν_1 and the sum of ν_2 and ν_3 show a clear anticorrelation in the three-dimensional JSI of triplet, but two of them do not show a specific type of correlation. Shalm *et al.* [24] have experimentally demonstrated genuine tripartite frequency-time entanglement between three separated particles.

B. Factorable tripartite frequency correlation

If the pump spectrum is not perfectly monochromatic, it is still true that energy is conserved in the PDC process, but

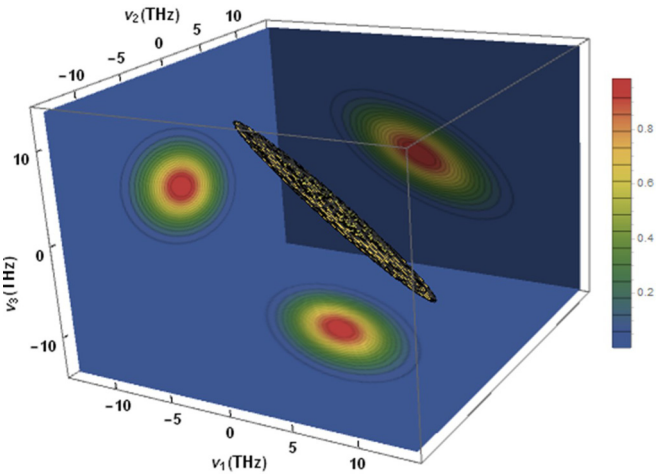

FIG. 3. JSI of the triplet and the corresponding projection between any two of the photons. ν_1 and the sum of ν_2 and ν_3 show a clear anticorrelation, but two photons of the triplet do not show a specific type of correlation.

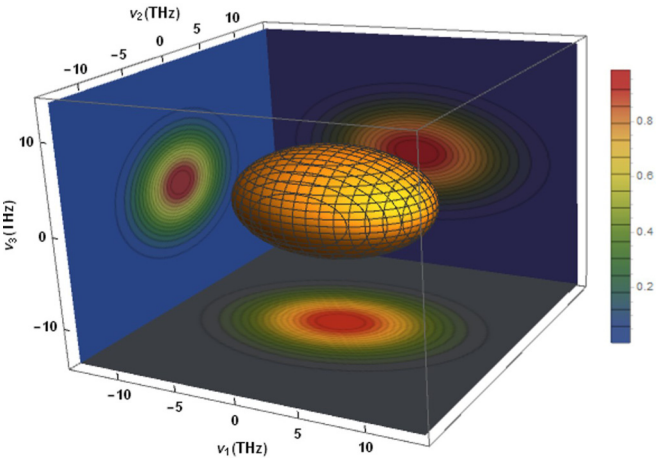

FIG. 4. The ellipsoid in the box represents the JSI of ν_1, ν_2, and ν_3. Projection of the ellipsoid on the bottom, left, and back sides exhibit no correlation between ν_1 and ν_2, ν_2 and ν_3, and ν_1 and ν_3, respectively.

the correlations are weakened due to the larger spread of the signal-idler sum frequencies, and the tripartite state shows a rich spectral structure. The property of correlation is governed on the one hand by the spectral pump distribution and on the other hand by the dispersive properties of the used crystal. By adapting the pump bandwidth and the corresponding group velocities of the pump and down-converted photons for specific crystal, it becomes possible that factorable tripartite frequency correlation can be generated.

According to Eq. (16), we can obtain a factorable tripartite correlation by eliminating the last two exponential terms; then we need to keep

$$\frac{2}{\sigma^2}+\frac{\gamma {L_1}^2 a_1 a_2}{2}=0,\ \frac{2}{\sigma^2}+\frac{\gamma {L_1}^2 a_2^2}{2}+\frac{\gamma {L_2}^2 b_1 b_2}{2}=0. \tag{18}$$

From the above equations, we can see that due to the constraints of group velocity, $a_1a_2<0, b_1b_2<0$ are required. The inequality $a_1a_2<0$ may be met either when $\mu_0<\mu_p<\mu_1$ or when $\mu_1<\mu_p<\mu_0$ in the first SPDC stage, and $\mu_2<\mu_0<\mu_3$ or $\mu_3<\mu_0<\mu_2$ should be satisfied for $b_1b_2<0$ in the second stage. That is to say, the group velocity of the pump ω_p and ω_0 in the two SPDC processes must lie between that of the two down-converted photons. For simplicity, we assume $a_1=-a_2$, $b_1=-b_2$, and when these GVM conditions are satisfied, the reciprocal group velocity of the pump is equal to the average of the signal and idler reciprocal group velocities, i.e., $2/\mu_p=1/\mu_0+1/\mu_1, 2/\mu_0=1/\mu_2+1/\mu_3$.

Since different nonlinear crystal have different dispersive properties of group velocity, after comparing the group velocity of different polarizations in several materials, we choose lithium niobate as the quadratic nonlinear crystal in our proposal, not only for the GVM conditions, but also for its large second-order nonlinear coefficient. Then we may give an example based on nondegenerate cascaded SPDC in periodically poled lithium niobate (PPLN) crystal. Two conditions of GVM are considered together; we can select the proper wavelength of the pump and the down-converted photons. In the first poled region, a pulsed laser beam at $\lambda_p=656$ nm serves as the pump and drives the type-I SPDC process ($e\rightarrow o+o$) in order to produce nondegenerate photon pairs at $\lambda_0=800.16$ and $\lambda_1=3641.14$ nm. By deploying the photon λ_0 again as the pump in the second type-I SPDC stage ($e\rightarrow o+o$), we can generate secondary down-converted photon pairs $\lambda_2=1390.46$ and $\lambda_3=1884.78$ nm. The GVM conditions in PPLN at the mentioned wavelengths are satisfied for both type-I processes. However, between the two processes, a electro-optic polarization converter [36] should be used to change the polarization state ($o\rightarrow e$) by applying a voltage to photons 0 and 1. After calculating the inverse of group velocity for these wavelengths, we know $a_1=-a_2=8.54\times10^{-11}\,(\mathrm{m/s})^{-1}$, $b_1=-b_2=1.62\times10^{-11}\,(\mathrm{m/s})^{-1}$. In this case, in order to cancel zeroth-order phase matching for the selected wavelength, the grating periods $\Lambda_1=16.29\ \mu$m and $\Lambda_2=20.56\ \mu$m are required. Then both the GVM and the conversional phase-matching condition are satisfied.

Under the EPM conditions, from Eq. (18) we know that if $\sigma L_1=5.33\times10^{10}$ (Hz m) and $\sigma L_2=3.97\times10^{11}$ (Hz m) are satisfied at the same time, ν_1, ν_2, and ν_3 will be fully uncorrelated. Then the JSA of the factorable tripartite can be written as

$$F(\nu_1)F(\nu_2)F(\nu_3)=e^{-\alpha\nu_1^2}e^{-\beta\nu_2^2}e^{-\eta\nu_3^2}. \tag{19}$$

For a pump field centered at 656 nm having a full width at half maximum (FWHM) bandwidth of 20 nm, the corresponding range of adjustable spectral bandwidth is 0–13.94 THz. We can plot the JSI of the tripartite state $|F(\nu_1,\nu_2,\nu_3)|^2$ with the selected parameters. For our PPLN example, in order to meet the conditions of no frequency correlation, it is feasible to select the pump bandwidth $\sigma=13.94$ THz; then the crystal can keep reasonable lengths of $L_1=3.82$ mm and $L_2=2.85$ cm. These parameters yield a ellipsoid JSI in a shape which represents the lack of correlation of ν_1, ν_2, and ν_3 as depicted in the box of Fig. 4. A nearly perfect circular frequency spectrum intensity is projected on the ν_2-ν_3 plane, which is fully uncorrelated between ν_2 and ν_3. Because of the symmetry of ν_2 and ν_3,

TABLE I. Relations between the relative bandwidths of pump function and phase-matching function in the cascaded SPDC processes, and the corresponding correlations they exhibit. σ is the pump bandwidth; L_1 and L_2 are the length of two SPDC areas.

Relations between ν_0 and ν_1 in SPDC1		
$\sigma \ll \frac{2}{\sqrt{\gamma}L_1 a_1}$	$\sigma \approx \frac{2}{\sqrt{\gamma}L_1 a_1}$	$\sigma \gg \frac{2}{\sqrt{\gamma}L_1 a_1}$
anticorrelated	uncorrelated	positively correlated
Correlation of ν_2 and ν_3 when ν_0 and ν_1 are uncorrelated		
$\sigma \ll \frac{2}{\sqrt{\gamma\left[b_1^2L_2^2-a_1^2L_1^2\right]}}$	$\sigma \approx \frac{2}{\sqrt{\gamma\left[b_1^2L_2^2-a_1^2L_1^2\right]}}$	$\sigma \gg \frac{2}{\sqrt{\gamma\left[b_1^2L_2^2-a_1^2L_1^2\right]}}$
anticorrelated	uncorrelated	positively correlated

both the projections on the ν_1-ν_2 plane and ν_1-ν_3 plane exhibit the same ellipse shape with slightly elongation along one axis. However, the range of frequencies expected for either photon in the circular contour or in the ellipse shape is independent of the frequency detected for its sibling.

C. Separable one photon and biphoton

In Subsec. B, we give the exact solution of Eq. (18) with the proper parameters. As discussed previously, we can also manipulate the tripartite frequency correlation by comparing the relative widths of the pump function and phase-matching function. We divided the discussion of separable tripartite frequency correlation into several steps.

First, we consider the correlation between the photons ω_1 and ω_0 produced in the first SPDC process. The bandwidth of phase-matching function $\delta\phi_1 = \frac{2}{\sqrt{\gamma}L_1 a_1}$ can be obtained from the expression of bipartite spectral function, and the pump bandwidth is σ. In order to eliminate frequency correlations in SPDC1, σ and $\delta\phi_1$ should be designed so as to ensure the bandwidths of the two functions are similar, i.e., $\sigma \approx \frac{2}{\sqrt{\gamma}L_1 a_1}$. However, in the first SPDC process ν_1 and ν_0 can be anticorrelated either by reducing the pump bandwidth σ or by increasing the crystal length L_1. And they can be positively correlated by increasing the pump bandwidth σ or by reducing the crystal length L_1. When there is no correlation between ν_1 and ν_0, and ν_0 splits into ν_2 and ν_3, the JSA of tripartite can be described as a separable one photon and biphoton

$$F(\nu_1)F(\nu_2,\nu_3) = e^{-A\nu_1^2}e^{-B(\nu_2+\nu_3)^2}e^{-C(\nu_2-\nu_3)^2}, \qquad (20)$$

where $A = 1/\sigma^2 + \gamma L_1^2 a_1^2/4$, $B = 1/\sigma^2 + \gamma L_1^2 a_1^2/4$, $C = \gamma L_2^2 b_1^2/4$. From the expression above, we can see that ν_1 is independent of ν_2 and ν_3, which can be traced out from the tripartite. Then we consider the correlation between photon pairs ω_2 and ω_3 generated in the second SPDC process. It is obvious that how the detuning frequencies ν_2 and ν_3 are correlated depends on the comparison between the bandwidths of two exponential functions which are related to B and C. When these two values are equal, i.e., $\sigma = 2/\sqrt{\gamma[b_1^2L_2^2 - a_1^2L_1^2]}$ is satisfied, ν_2 and ν_3 can be uncorrelated. As we can see from this formula, the correlation is not only related to σ and L_1, but also it can be manipulated by varying the length L_2. Relations between the pump bandwidth σ and other parameters are listed in Table I as well as the corresponding correlations they exhibit.

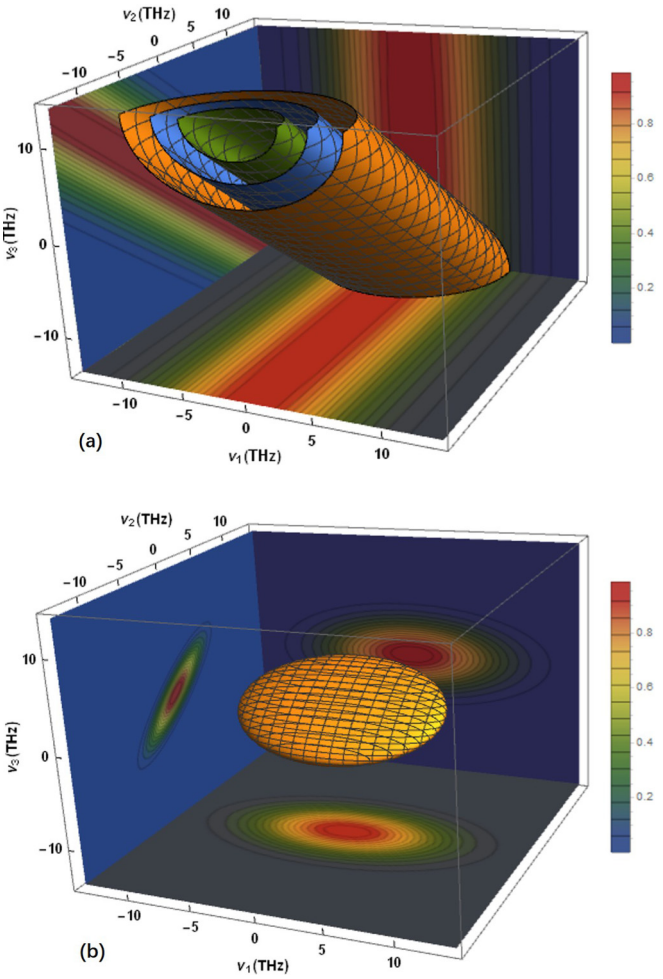

FIG. 5. Manipulation of frequency correlation between ν_2 and ν_3 by varying the length of L_2 when ν_0 are uncorrelated with ν_1, in both panels (a) and (b), $\sigma = 13.94$ THz and $L_1 = 3.82$ mm. (a) $L_2 = 1$ mm; anticorrelation between ν_2 and ν_3 is exhibited. (b) $L_2 = 10$ cm; positive correlation between ν_2 and ν_3 is exhibited.

By combining the two SPDC processes together, we can select $\sigma = 13.94$ THz as a fixed value since both processes share a common pump bandwidth, and the crystal length is set to $L_1 = 3.82$ mm and $L_2 = 2.85$ cm. In this case, the conditions for lack of correlation for two processes can be met simultaneously. Given a specific down-converted event in the first (second) stage, we can manipulate the frequency correlation between ν_2 and ν_3 (ν_0 and ν_1) by changing L_2 (L_1), respectively. For example, if we keep $L_1 = 3.82$ mm unchanged, but L_2 is reduced to 1 mm, then the JSI between ν_2 and ν_3 will exhibit anticorrelation distribution while it remains uncorrelated between ν_1 and ν_0 (sum of ν_2 and ν_3) which can be observed from the contour of three-dimension graphics and projections in Fig. 5(a). If the length of L_2 is increased to 10 cm, then the JSI of ν_2 and ν_3 will exhibit frequency positive-correlation contour as shown in Fig. 5(b). Another case is of particular interest, when it is uncorrelated of ν_2 and ν_3 generated in the second SPDC process, but it is positively correlated or anticorrelated of ν_0 and ν_1 in the first process. We can herald the generation of photon pairs ω_1 and $\omega_3(\omega_2)$ in the corresponding correlation deterministically

by the measurement of photon at frequency $\omega_2(\omega_3)$; this is very important and interesting because it provides a source of heralded correlation photon pairs for quantum communication and processing applications.

IV. CONCLUSION

In this paper, we investigate manipulation of tripartite frequency correlation under EPM conditions in a monolithic quadratic nonlinear crystal. Based on PPLN crystal waveguide, we designed a cascaded periodically poled structure for two nondegenerate SPDC processes. According to our analysis, by adjusting the crystal length of two different segments and the bandwidth of pulse pump laser, the frequency spectrum will show a full correlation, partial correlation, or no correlation, corresponding to a fully inseparable triplet, separable one photon and biphoton, or three separable photons, respectively. Fully inseparable triplet implies genuine tripartite entanglement, which is suitable for three-party quantum secret sharing. Separable one photon and biphoton can be used to herald the entangled photon pairs deterministically but without postselection. Three separable photons are valuable resources in multiphoton boson sampling experiment, which is a promising approach to obtain evidence of quantum supremacy. These approaches proposed for manipulation of frequency correlation in a single crystal may provide useful tools for the management of multipartite entanglement in quantum communication and networking.

ACKNOWLEDGMENTS

We would like to thank Profs. Q. Y. He and X. S. Ma for helpful discussion. This work was supported by National Key R&D Program of China (No. 2017YFA0303700) and National Natural Science Foundation of China (Contracts No. 11621091, No. 11627810, No. 11690031, No. 11474050, and No. 11674169). Z.D.X. appreciates the support from the National Young 1000 Talent Plan.

[1] K. Modi, T. Paterek, W. Son, V. Vedral, and M. Williamson, Unified View of Quantum and Classical Correlations, Phys. Rev. Lett. **104**, 080501 (2010).

[2] N. Gisin, G. Ribordy, W. Tittel, and H. Zbinden, Quantum cryptography, Rev. Mod. Phys. **74**, 145 (2002).

[3] L. Upton, M. Harpham, O. Suzer, M. Richter, S. Mukamel, and T. Goodson, Optically excited entangled states in organic molecules illuminate the dark, J. Phys. Chem. Lett. **4**, 2046 (2013).

[4] W. P. Grice, A. B. U'Ren, and I. A. Walmsley, Eliminating frequency and space-time correlations in multiphoton states, Phys. Rev. A **64**, 063815 (2001).

[5] O. Kuzucu, F. N. C. Wong, S. Kurimura, and S. Tovstonog, Joint Temporal Density Measurements for Two-Photon State Characterization, Phys. Rev. Lett. **101**, 153602 (2008).

[6] P. J. Mosley, J. S. Lundeen, B. J. Smith, P. Wasylczyk, A. B. U'Ren, C. Silberhorn, and I. A. Walmsley, Heralded Generation of Ultrafast Single Photons in Pure Quantum States, Phys. Rev. Lett. **100**, 133601 (2008).

[7] V. Giovannetti, S. Lloyd, and L. Maccone, Quantum-enhanced positioning and clock synchronization, Nature (London) **412**, 417 (2001).

[8] V. Giovannetti, L. Maccone, J. H. Shapiro, and F. N. C. Wong, Generating Entangled Two-Photon States with Coincident Frequencies, Phys. Rev. Lett. **88**, 183602 (2002).

[9] O. Kuzucu, M. Fiorentino, M. A. Albota, F. N. C. Wong, and F. X. Kärtner, Two-Photon Coincident-Frequency Entanglement via Extended Phase Matching, Phys. Rev. Lett. **94**, 083601 (2005).

[10] D. E. Browne and T. Rudolph, Resource-Efficient Linear Optical Quantum Computation, Phys. Rev. Lett. **95**, 010501 (2005).

[11] M. Gimeno-Segovia, P. Shadbolt, D. E. Browne, and T. Rudolph, From Three-Photon Greenberger-Horne-Zeilinger States to Ballistic Universal Quantum Computation, Phys. Rev. Lett. **115**, 020502 (2015).

[12] M. Hillery, V. Bužek, and A. Berthiaume, Quantum secret sharing, Phys. Rev. A **59**, 1829 (1999).

[13] A. M. Lance, T. Symul, W. P. Bowen, B. C. Sanders, and P. K. Lam, Tripartite Quantum State Sharing, Phys. Rev. Lett. **92**, 177903 (2004).

[14] X. C. Yao, T. X. Wang, P. Xu, H. Lu, G. S. Pan, X. H. Bao, C.-Z. Peng, C.-Y. Lu, Y.-A. Chen, and J.-W. Pan, Observation of eight-photon entanglement, Nat. Photon. **6**, 225 (2012).

[15] X.-L. Wang, L.-K. Chen, W. Li, H.-L. Huang, C. Liu, C. Chen, Y.-H. Luo, Z.-E. Su, D. Wu, Z.-D. Li, H. Lu, Y. Hu, X. Jiang, C.-Z. Peng, L. Li, N.-L. Liu, Y.-A. Chen, C.-Y. Lu, and J.-W. Pan, Experimental Ten-Photon Entanglement, Phys. Rev. Lett. **117**, 210502 (2016).

[16] A. Politi, J. C. F. Matthews, and J. L. O'Brien, Shor's quantum factoring algorithm on a photonic chip, Science **325**, 1221 (2009).

[17] A. M. Childs, D. Gosset, and Z. Webb, Universal computation by multiparticle quantum walk, Science **339**, 791 (2013).

[18] M. A. Broome, A. Fedrizzi, S. Rahimi-Keshari, J. Dove, S. Aaronson, T. C. Ralph, and A. G. White, Photonic boson sampling in a tunable circuit, Science **339**, 794 (2013).

[19] J. B. Spring, B. J. Metcalf, P. C. Humphreys, W. S. Kolthammer, X. M. Jin, M. Barbieri, A. Datta, N. Thomas-Peter, N. K. Langford, D. Kundys, J. C. Gates, B. J. Smith, P. G. R. Smith, and I. A. Walmsley, Boson sampling on a photonic chip, Science **339**, 798 (2013).

[20] M. Tillmann, B. Dakic, R. Heilmann, S. Nolte, A. Szameit, and P. Walther, Experimental boson sampling, Nat. Photon. **7**, 540 (2013).

[21] A. Crespi, R. Osellame, R. Ramponi, D. J. Brod, E. F. Galvao, N. Spagnolo, C. Vitelli, E. Maiorino, P. Mataloni, and F. Sciarrino, Integrated multimode interferometers with arbitrary designs for photonic boson sampling, Nat. Photon. **7**, 545 (2013).

[22] H. Hübel, D. R. Hamel, A. Fedrizzi, S. Ramelow, K. J. Resch, and T. Jennewein, Direct generation of photon triplets using cascaded photon-pair sources, Nature (London) **466**, 601 (2010).

[23] D. M. Greenberger, M. A. Horne, A. Shimony, and A. Zeilinger, Bell's theorem without inequalities, Am. J. Phys. **58**, 1131 (1990).

[24] L. K. Shalm, D. R. Hamel, Z. Yan, C. Simon, K. J. Resch, and T. Jennewein, Three-photon energy-time entanglement, Nat. Phys. **9**, 19 (2012).

[25] S. Agne, T. Kauten, J. Jin, E. Meyer-Scott, J. Z. Salvail, D. R. Hamel, K. J. Resch, G. Weihs, and T. Jennewein, Observation of Genuine Three-Photon Interference, Phys. Rev. Lett. **118**, 153602 (2017).

[26] D. R. Hamel, L. K. Shalm, H. Hübel, A. J. Miller, F. Marsili, V. B. Verma, R. P. Mirin, S. W. Nam, K. J. Resch, and T. Jennewein, Direct generation of three-photon polarization entanglement, Nat. Photon. **8**, 801 (2014).

[27] S. Krapick, B. Brecht, H. Herrmann, V. Quiring, and C. Silberhorn, On-chip generation of photon-triplet states, Opt. Express **24**, 2836 (2016).

[28] M. G. Moebius, F. Herrera, S. Griesse-Nascimento, O. Reshef, C. C. Evans, G. G. Guerreschi, A. Aspuru-Guzik, and E. Mazur, Efficient photon triplet generation in integrated nanophotonic waveguides, Opt. Express **24**, 9932 (2016).

[29] M. Corona, K. Garay-Palmett, and A. B. U'Ren, Third-order spontaneous parametric down-conversion in thin optical fibers as a photon-triplet source, Phys. Rev. A **84**, 033823 (2011).

[30] H. Y. Leng, X. Q. Yu, Y. X. Gong, P. Xu, Z. D. Xie, H. Jin, C. Zhang, and S. N. Zhu, On-chip steering of entangled photons in nonlinear photonic crystals, Nat. Commun. **2**, 429 (2011).

[31] Y. X. Gong, Z. D. Xie, P. Xu, X. Q. Yu, P. Xue, and S. N. Zhu, Compact source of narrow-band counterpropagating polarization-entangled photon pairs using a single dual-periodically-poled crystal, Phys. Rev. A **84**, 053825 (2011).

[32] H. Jin, P. Xu, X. W. Luo, H. Y. Leng, Y. X. Gong, W. J. Yu, M. L. Zhong, G. Zhao, and S. N. Zhu, Compact Engineering of Path-Entangled Sources from a Monolithic Quadratic Nonlinear Photonic Crystal, Phys. Rev. Lett. **111**, 023603 (2013).

[33] Z. D. Xie, T. Zhong, S. Shrestha, X. A. Xu, J. L. Liang, Y. X. Gong, J. C. Bienfang, A. Restelli, J. H. Shapiro, F. N. C. Wong, and C. W. Wong, Harnessing high-dimensional hyperentanglement through a biphoton frequency comb, Nat. Photon. **9**, 536 (2015).

[34] W. P. Grice and I. A. Walmsley, Spectral information and distinguishability in type-II down-conversion with a broadband pump, Phys. Rev. A **56**, 1627 (1997).

[35] J. P. Torres, F. Macià, S. Carrasco, and L. Torner, Engineering the frequency correlations of entangled two-photon states by achromatic phase matching, Opt. Lett. **30**, 314 (2005).

[36] C. Y. Huang, C. H. Lin, Y. H. Chen, and Y. C. Huang, Electro-optic Ti:PPLN waveguide as efficient optical wavelength filter and polarization mode converter, Opt. Express **15**, 2548 (2007).